Kovove Mater. 64 2026 1–12
DOI: 10.31577/km.2026.1.1

Influencing impact toughness transition temperatures of high carbon powder metallurgy steels by nickel adding

Tuğba Bilgin[1,2]*, Onur Altuntaş[3], Ahmet Güral[4]

[1] *Gazi University Graduate School of Natural and Applied Sciences, Department of Metallurgical and Materials Engineering Ankara, Turkey*
[2] *VOLO Composite and Engineering LTD., 06890 Kahramankazan, Ankara, Turkey*
[3] *National Defense University, Alparslan Defense Sciences and National Security Institute, Department of Warfare Weapons and Tools, Ankara, Turkey*
[4] *Gazi University Faculty of Technology, Department of Metallurgical and Materials Engineering Ankara, Turkey*

Received 05 March 2025, received in revised form 16 July 2025, accepted 25 July 2025

Abstract

The aim of the study is to investigate the effects on impact toughness properties of powder metallurgy (P/M) steels depending on different nickel ratios. For this purpose, ferrous P/M alloy samples containing 1.2 wt.% carbon and different nickel contents (0.5–5 wt.%) were compacted under 700 MPa pressure and sintered at 1200 °C under 5×10^{-2} Pa vacuum atmosphere. Following sintering, the densification rate and macrohardness (HV2) measurements of the samples were carried out. Fracture morphologies of the samples having different nickel content following impact toughness tests at various temperature (–40 to 40 °C) were imaged by scanning electron microscopy (SEM). Metallurgical characterizations of the samples with different nickel content were analyzed SEM and X-ray diffractometer (XRD). It was understood that pearlitic transformation was suppressed with the formation of nickel-rich austenitic areas in the microstructure of nickel-doped P/M steels. The hardness and impact toughness values of PM steel samples with 5 % nickel addition were increased by approximately 121 and 247 %, respectively, compared to samples without nickel addition, at all test temperatures.

K e y w o r d s: powder metallurgy steel, nickel, impact transition temperature, microstructure and hardness

1. Introduction

Nowadays Powder Metallurgy (P/M) steels have a wide range of applications. However, it is insufficient for some uses due to its low mechanical properties [1]. In order to increase the use of P/M steels in places requiring high performance, it is necessary to improve their mechanical properties. One of the mechanical properties of P/M steels that needs to be improved is the impact toughness values, which are conditions under dynamic loads. One of the methods applied to improve the mechanical properties is the addition of alloying elements. Since the alloying elements will affect the sintering kinetics, shrinkage behavior and sinterability, the properties of the alloying elements to be added should be well known. Alloying elements added to P/M steels should be chosen not only on the basis of the desired strength, but also taking into account their dimensional stability during sintering [2, 3]. With the increase of the carbon content in the steels, the hardness, and yield stress of the steels increase, while the impact strength and ductility decrease [4, 5].

The addition of nickel improves the mechanical properties of P/M steel components by increasing strength, impact resistance, wear resistance and fatigue performance. Addition of nickel to P/M steels reduces the porosity rate due to the shrinkage effect [6, 7]. In addition, nickel has a lower diffusion coefficient compared to many elements and diffuses more slowly into iron [8]. Addition of nickel to P/M steel results in the formation of nickel-rich areas (NRA). The presence of NRA is usually explained by the slow diffusion of nickel to iron. [9].

The presence of nickel promotes the formation of

*Corresponding author: e-mail address: tugba.bilgin@gazi.edu.tr

Table 1. Density and concentration ratio values of P/M samples after pressing and sintering

	0 % Ni	0.5 % Ni	1 % Ni	2 % Ni	5 % Ni
Green density ($g\,cm^{-3}$)	6.58	6.65	6.72	6.90	6.93
Sintered density ($g\,cm^{-3}$)	6.81	6.88	6.91	7.11	7.15
Densification ratio (%)	87.0	88.2	88.5	91.1	91.6

a protective oxide layer on the material's surface, enhancing its resistance to corrosive environments. Nickel-rich areas can lead to enhanced toughness and ductility. This is due to several factors, including solid solution strengthening and the prevention of dislocation movement. These effects hinder crack propagation and promote plastic deformation prior to fracture [10].

In the present study, the effects of adding different amounts of nickel on the impact transition temperatures of PM steels containing 1.2 wt.% C were examined. Investigating the toughness properties of nickel-containing PM steels depending on the impact transition temperature together with microstructural transformations is expected to provide important information for other studies in the relevant field.

2. Experimental procedures

In experimental studies, in order to produce nickel-added high-carbon powder metallurgy (P/M) steel samples, 1.2 % by weight natural graphite powders (Alpha) as carbon addition to pure iron powders having 99.9 % purity and 5 μm particle size produced by electrolysis production method. Powder mixtures were prepared by adding 0.5-1-2-5 wt.% nickel powders having 3–7 μm size 0.5 wt.% Zn Stearate was used as a lubricant. The homogeneously mixed powders were pressed in a single-acting hydraulic pressing device at room temperature under 700 MPa pressure in accordance with ASTM B 243-94 standard. Green density samples were produced as unnotch impact test samples in a mold in accordance with ISO-5754 standard. In order to strengthen the green density samples, sintering was carried out in an alumina tube by keeping them in a vacuum atmosphere of 5×10^{-2} Pa at 1200 ℃ for 30 minutes. After pressing and sintering processes, the density calculations of the samples were measured on an A&D HR-250AZ brand precision balance with a sensitivity of 10^{-4} g according to the Archimedean principle in accordance with ASTM B962-17 standard.

Conventional metallographic processes of the sintered P/M samples were applied for microstructure analysis. For this purpose, following sanding with SiC particles (80–2500 #), all samples were polished with a 3–1 μm diamond suspension in order to obtain a clear image without scratches. Each sample was etched in 3 % nital solution (3 ml HNO_3-100 ml ethanol) in order to obtain a microstructure image after the polishing process. Surface and fractured surface examinations of the samples were carried out using JEOL JSM-6060LV Scanning Electron Microscope (SEM). X-ray analysis was applied to determine the precipitated phases in the alloy. In this technique, analysis was performed using CuKα probe with $\lambda = 1.5406$ and $0.5^\circ\,min^{-1}$ scanning speed. The hardness measurements of the samples were determined by macro hardness measurements (HV2) in Duravision 2000 Emco brand hardness device using 2 kg load in accordance with ASTM E92-17 standards. The hardness measurements of the samples were performed from at least five different points, and the arithmetic average was calculated. The impact tests of the samples were made by Instron-Wolpert impact tester device having 300 J hammer capacity. In order to examine the impact toughness behavior and hardness measurements up to –40 ℃ temperatures, Jinan Hensgrand Instrument Co. trademark DWC-80 model cooling cabinet is used. For the high temperature test at 40 ℃, laser thermometer-controlled pulse toughness tests of the samples placed in the helical structure were carried out. It was applied on at least 3 impact test samples for each different parameter.

3. Results and discussion

When the green densities of the samples produced after pressing and the sintering densities of the samples sintered in vacuum environment are compared, it is seen that the sintering density increases as seen in Table 1. There is porosity in the materials produced by the traditional P/M method [11]. The presence of pores causes the density of the produced samples to be lower than the theoretical density. There is an increase in the density values with the increase of nickel alloying element added to the samples. The presence of pores causes the density of the produced samples to be lower than the theoretical density. There is an increase in the density values with the increase of nickel alloying element added to the samples.

Typical lamellar pearlitic structures were observed in the microstructure image of the sintered sample, which was produced by adding 1.2 wt.%. graphite to the pure iron powder, as seen in Fig. 1a. The effects of

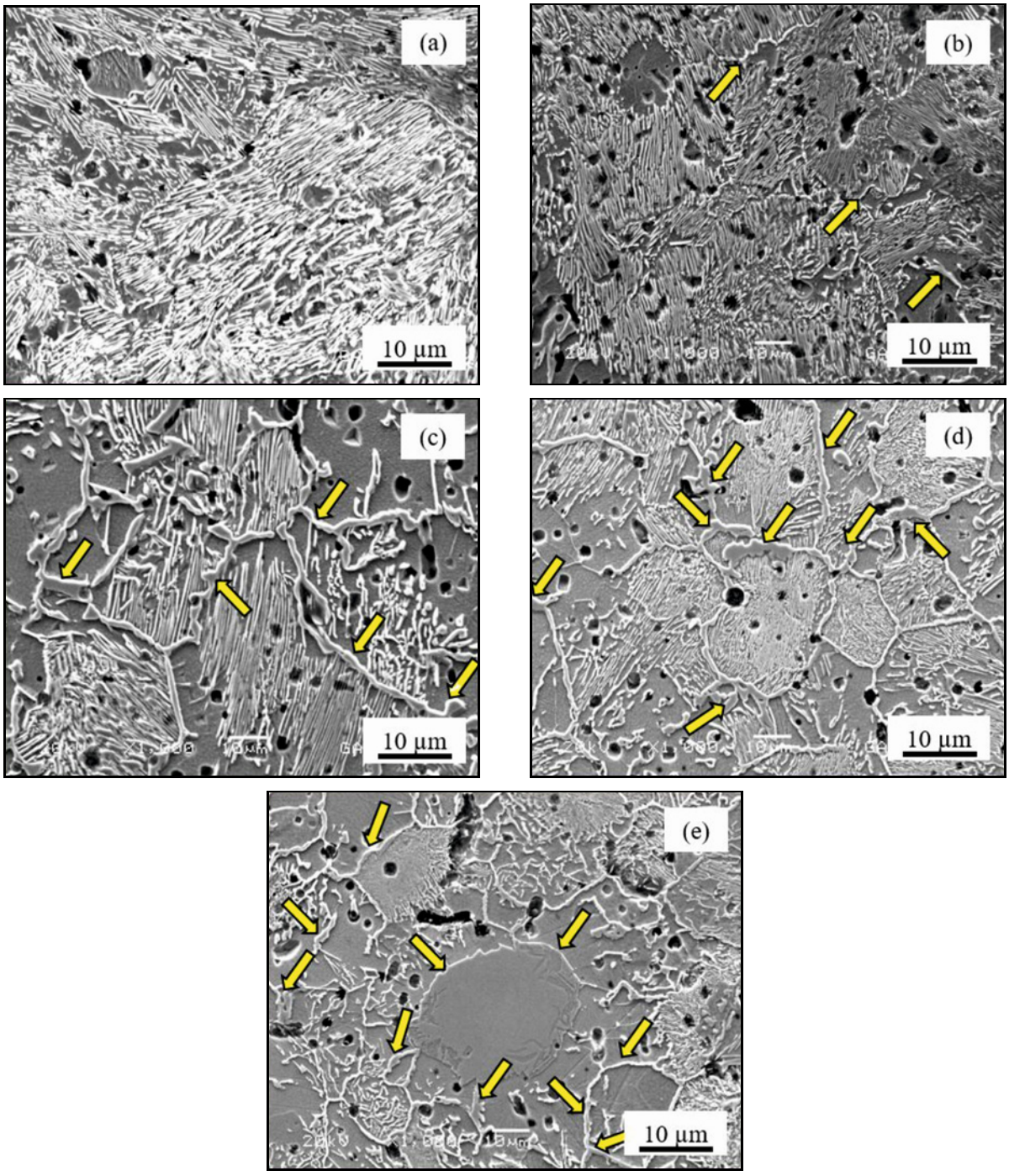

Fig. 1. SEM microstructure images of the sintered P/M steels: (a) 0 % Ni, (b) 0.5 % Ni, (c) 1% Ni, (d) 2 % Ni, and (e) 5 % Ni.

nickel, one of the alloying elements commonly added to steels, on the microstructure have been observed. As an alloying element, nickel expands the austenite region and narrows the ferrite region and has austenite stabilizing properties [11, 12]. Figures 1a–e show the SEM microstructure images of the samples to which (b) 0.5% nickel, (c) 1 % nickel, (d) 2 % nickel, and (e) 5 % nickel were added, respectively. As seen in Fig. 1, it was observed that the pearlite colony sizes decreased with the increase in the amount of nickel reinforcement in the structure. In addition, it can be clearly seen that the nickel-rich areas increase with the increase in the nickel ratio (indicated by the arrow). It is thought that pearlite colony ratios decrease with the addition of nickel, due to the conversion of these regions to the FCC crystal structure and possibly more dissolution of C atoms. [13].

Figure 2 shows the SEM image and EDS analysis of the sample containing 5 % nickel at 500× magnification. According to the elemental analysis of the 1st

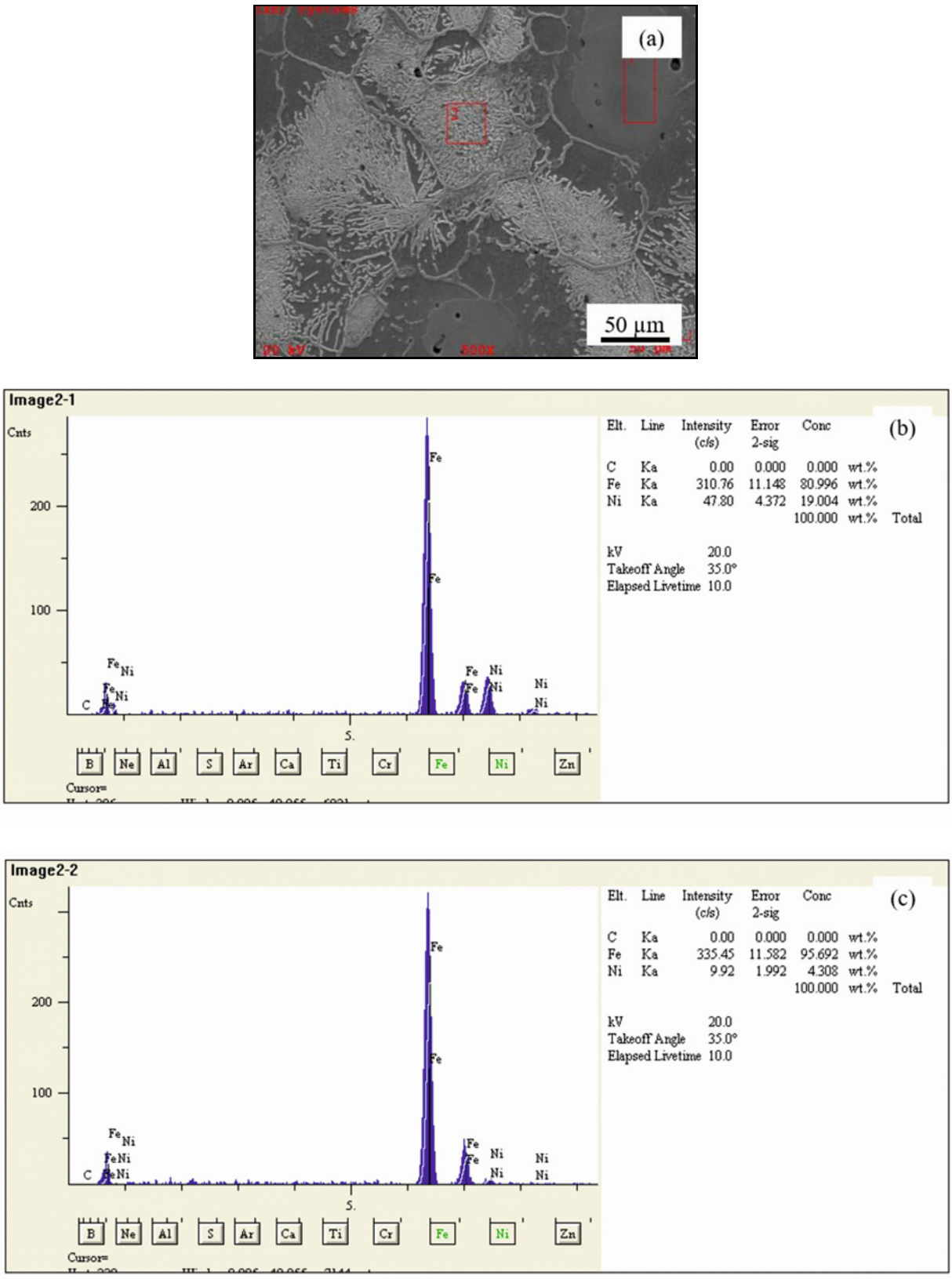

Fig. 2a–c. EDS analysis of the sintered P/M steel having 5 % nickel: (a) SEM microstructure images, (b) analysis of the first region, (c) analysis of the second region.

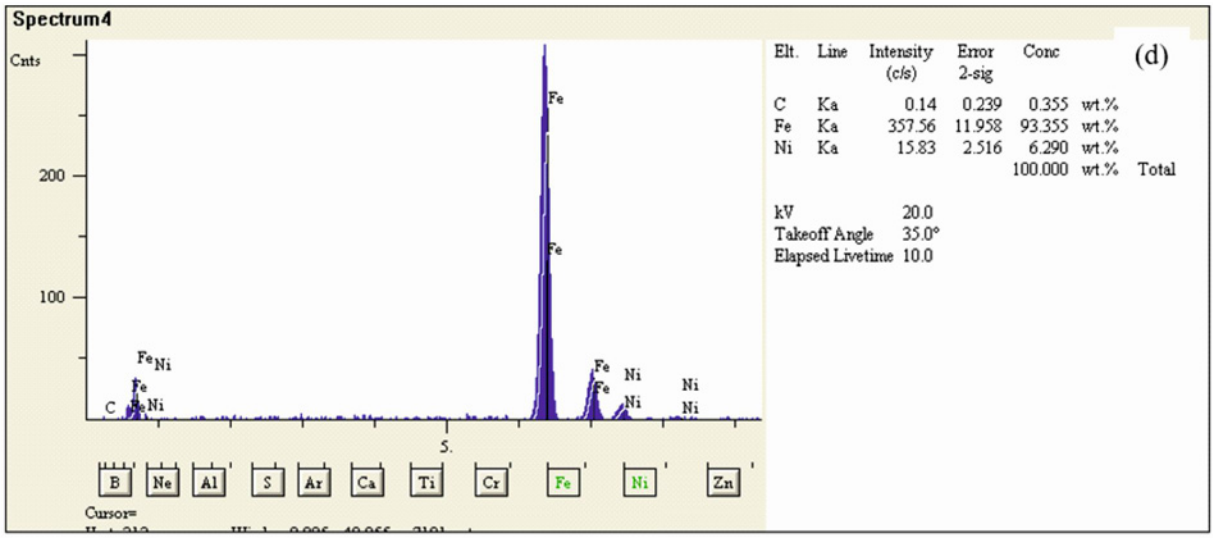

Fig. 2d. EDS analysis of the sintered P/M steel having 5 % nickel: (d) analysis of the SEM image area.

region on the SEM image (Fig. 2a), it is understood that the nickel rate is high outside the pearlitic area. Figure 1b shows that the EDS result shows that the nickel element ratio is 19 %. Therefore, it shows that these regions are nickel-rich. The reason for the high nickel content in nickel-rich regions is thought to be due to the low solid state diffusion time at the sintering temperatures of nickel powders added to iron and also the low solubility limit of nickel in iron.

In Fig. 2c, it is seen that the Ni content of the pearlitic region is lower, according to the EDS element analysis. The probable reason for this is that during sintering, the cementite phases that form pearlite colonies must nucleate and grow at iron grain boundaries with low nickel content. For the formation of Fe_3C, which is cementite, iron regions with low nickel content are needed. If the regions with high nickel content will transform the BCC iron phase into the FCC crystal structure, Fe_3C nucleation is not expected in the FCC iron regions. For this reason, it is seen in the iron phase outside the pearlite colonies of nickel-rich regions.

Figure 2d shows that there is 5 % nickel in the SEM image area according to EDS elemental analysis. This is an approximate value for the amount of nickel added. On the other hand, the reason why the value of carbon element analysis cannot be taken in EDS analyzes is that the values of elements with very small atomic radius such as carbon cannot be taken exactly in EDS element analysis.

The hardness values of the samples with different nickel reinforcement ratios were measured under the temperature variables at room temperature (21 °C) and –40 °C. It was observed that NRA increased in the samples with the increase of nickel ratio. The hardness value of the P/M samples without nickel addition at room temperature was increased from 84 to 186 HV2

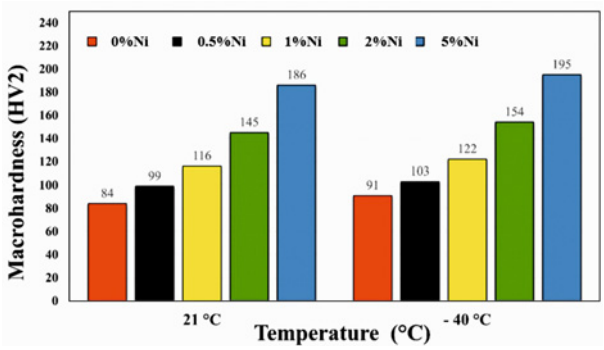

Fig. 3. The hardness values of P/M samples produced by adding different amounts of Ni in the temperature range of 21 and –40 °C.

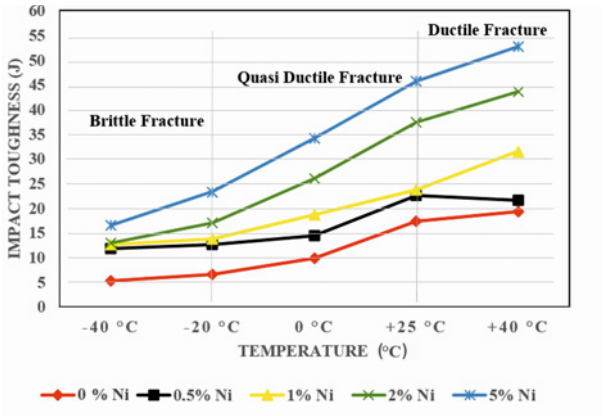

Fig. 4. Graph of impact toughness values (J) and transition temperature of powder metal samples produced by adding Ni at different rates.

of the sample containing 5 % nickel. In addition, an increase in the macrohardness values of the samples is

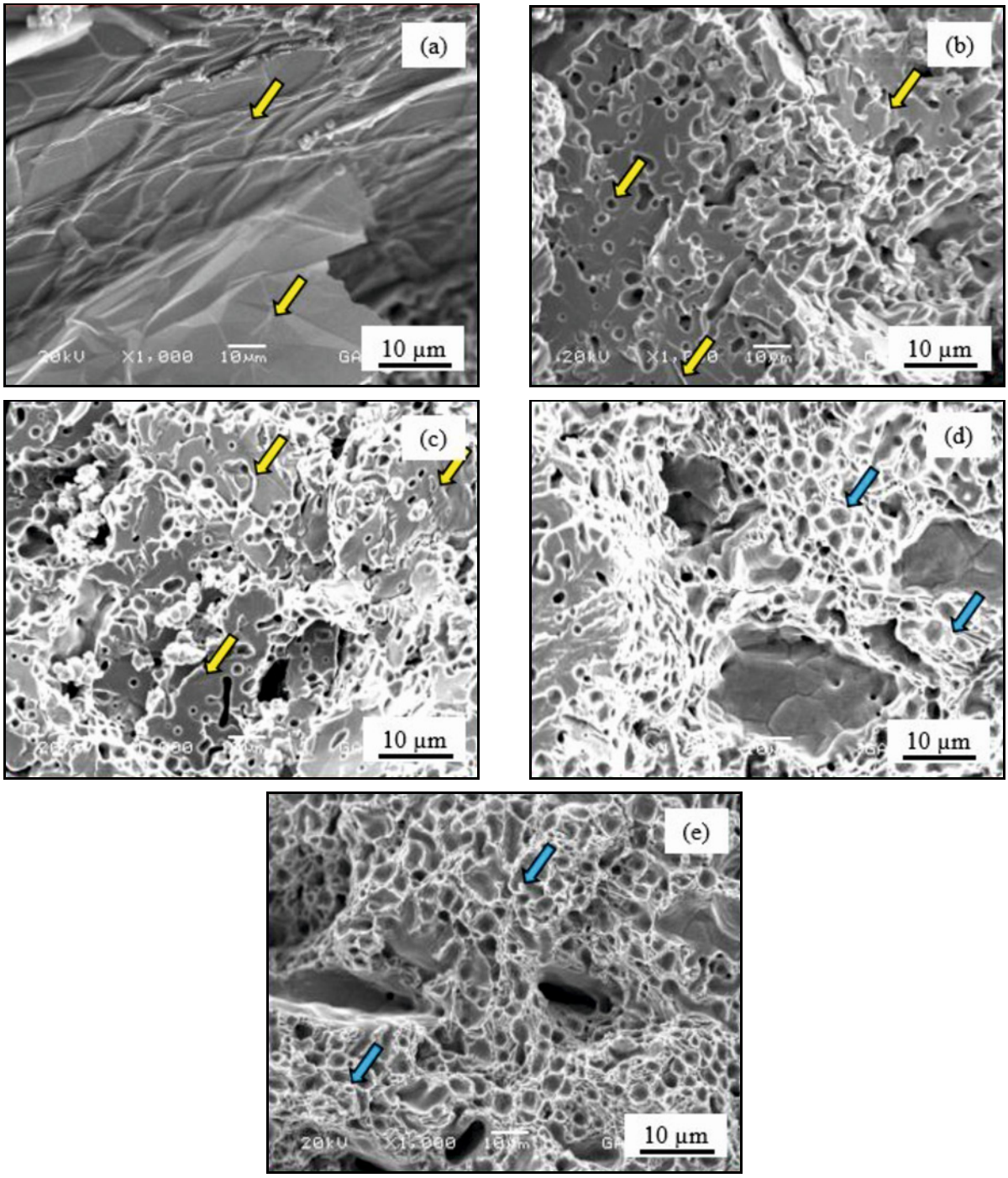

Fig. 5. Fractured surface SEM microstructures of the sample without Ni addition after impact test at different temperatures: (a) –40 °C, (b) –20 °C, (c) 0 °C, (d) 25 °C, and (e) 40 °C.

observed with the decrease in temperature. The hardness value of P/M steel without nickel addition increased from 91 HV2 at –40 °C, with increasing nickel ratio, the hardness of the sample containing 5 % nickel by weight increased up to 195 HV2. The variation of the hardness values of the samples at room temperature (21 °C) and –40 °C depending on the increasing nickel content by weight is presented in Fig. 3.

In the SEM microstructures in Fig. 1, the primary cementite networks in the structure became evident with the increase in the amount of nickel added. In addition to the prominence of the primary cementite networks, the length of the pearlite lamellae shortened and NRA increased. At the same time, NRA can be considered as the solid solution phase. This solid solution phase is not stoichiometric (stable) and may behave like an interphase. Therefore, an increase in hardness values was observed [14, 15].

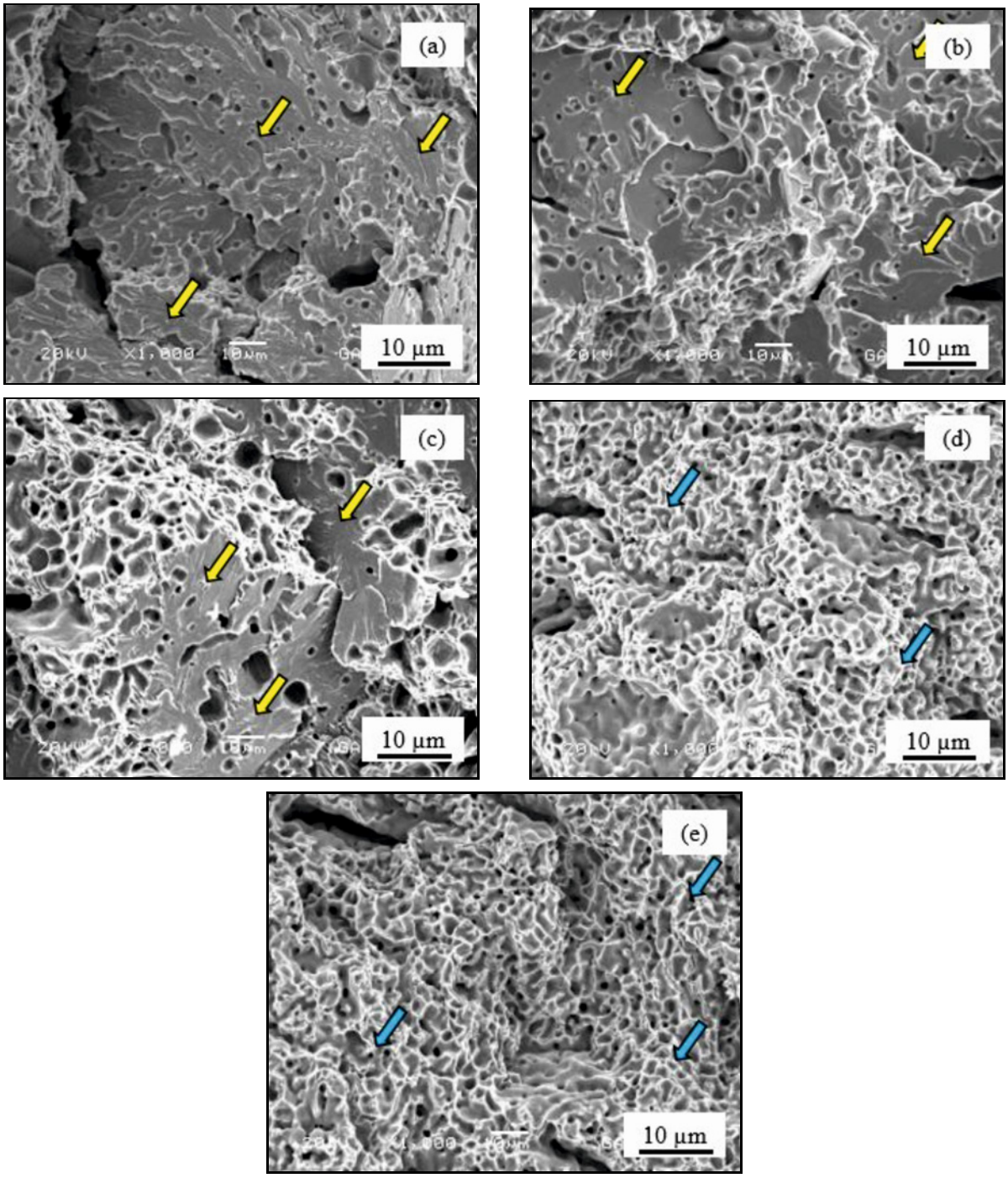

Fig. 6. Fractured surface SEM microstructures after impact toughness test at different temperatures of 0.5 % Ni by weight: (a) –40 °C, (b) –20 °C, (c) 0 °C, (d) 25 °C, and (e) 40 °C.

Engineering materials are not always used at room temperature conditions, sometimes at sub-zero temperatures and often even at temperatures above room temperature. For this reason, the temperature range of –40 and 40 °C, which can be used in industrial applications, was chosen in this study. As a result of experimental determinations, with the increase of nickel addition, the impact toughness energies of the samples increased at all temperatures (–40 to 40 °C) as seen in Fig. 5, the lowest toughness value was measured as 5.30 J in the sample without nickel addition at –40 °C, while this value was measured as 19.30 J in the same sample at 40 °C. With the addition of nickel, this value increased up to 52.70 J at 40 °C. Due to the dense shear plane family and high coordination number of FCC crystal structures, NRA contributes to the increase of ductility values, especially in dynamic loads, as it has lower shear stress without twinning deformation

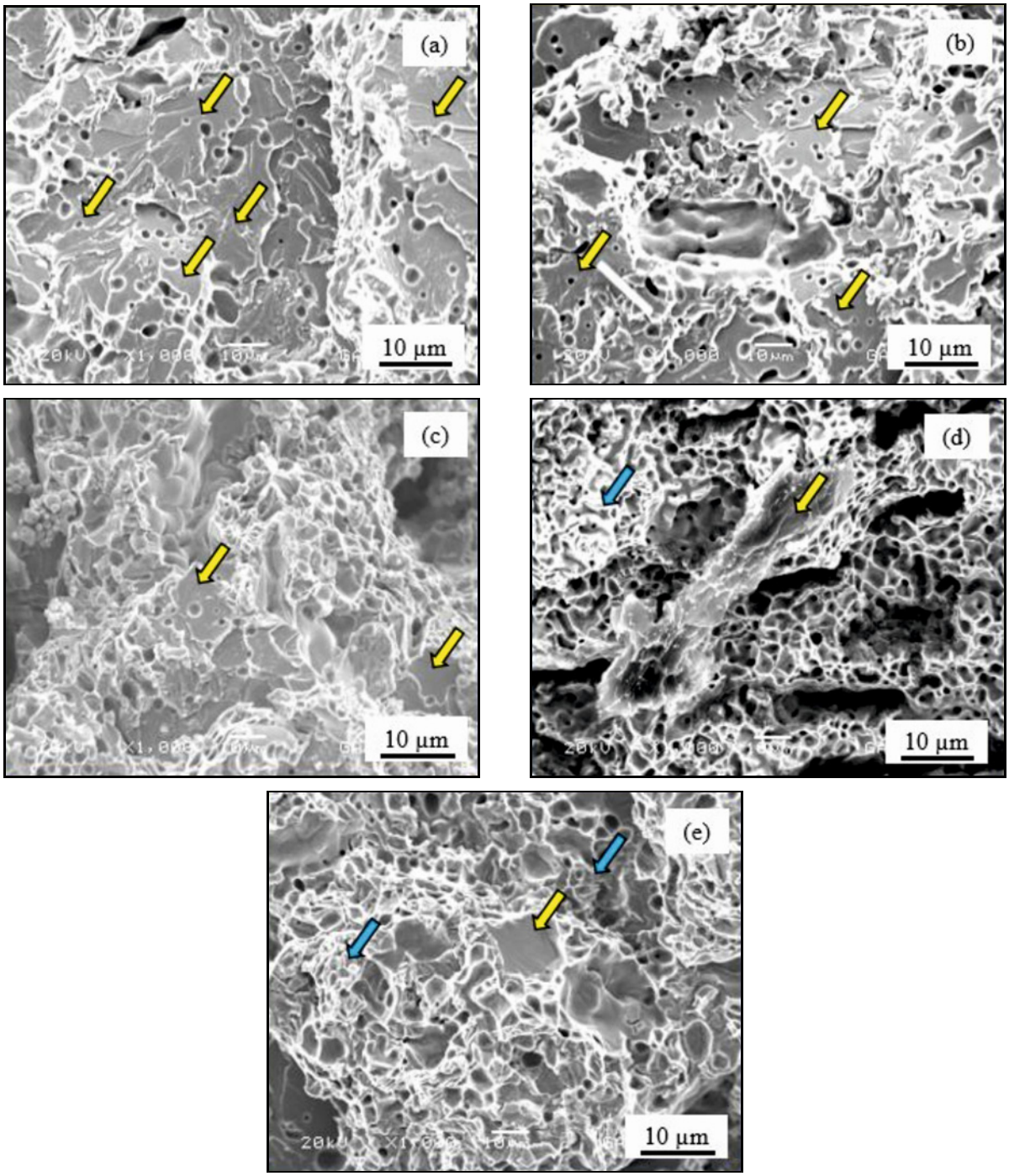

Fig. 7. Fractured surface SEM microstructures after impact test at 1 % by weight Ni at different temperatures: (a) –40 °C, (b) –20 °C, (c) 0 °C, (d) 25 °C, and (e) 40 °C.

mechanism [16, 17]. This situation is more effective in the {111} family and <110> family of direction in the FCC system. For this reason, it is expected that the impact resistance will be high in FCC crystalline materials. It is also known that FCC crystal structures have high impact resistance even at low temperatures. In this study, considering the impact toughness of the samples at the same temperatures the impact resistance of samples with 5 % nickel addition at temperatures of –40, –20, 0, 25, and 40 °C was increased by 311 %, respectively, compared to the sample without nickel addition. Impact transition temperature graphs in Fig. 4 were obtained by performing impact tests at different temperature parameters (–40, –20, 0, 25, and 40 °C).

After the impact toughness test, the fracture surfaces of the samples were examined with the SEM device and the fracture types were determined. Impact

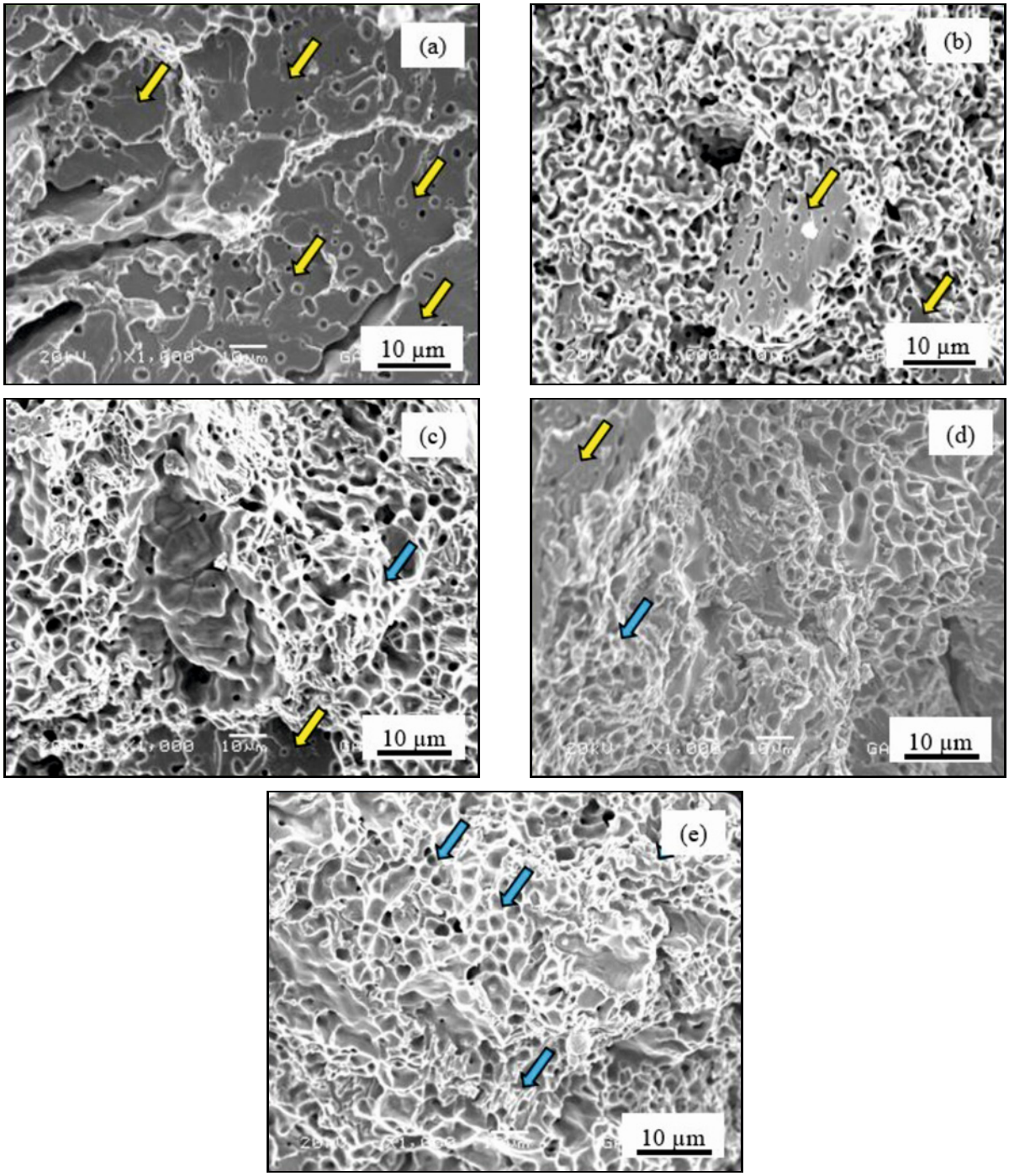

Fig. 8. Fractured surface SEM microstructures after impact test at 2 % by weight Ni at different temperatures: (a) –40 °C, (b) –20 °C, (c) 0 °C, (d) 25 °C, and (e) 40 °C.

test fracture surfaces containing different amounts of nickel and at different temperatures are shown in the figures below (Figs. 5–9). When the SEM microstructure images of the fracture surfaces of the sample without nickel addition in Figure 5 were examined after the impact test, the fracture surface progressed from brittle fracture to ductile rupture from –40 to 40 °C. It can be noted that the fracture surface morphologies and impact toughness values of the samples are compatible depending on the temperature increase. As the temperature increases, ductile rupture becomes more common, and a linear increase in impact toughness values is observed. In this sample without nickel addition, it can be seen that while the cleavage fracture mode is completely dominant at the places indicated by the yellow arrows at –40 °C, it decreases with the increase of the test temperature. Partially cleavage fracture modes were observed even at room temperature

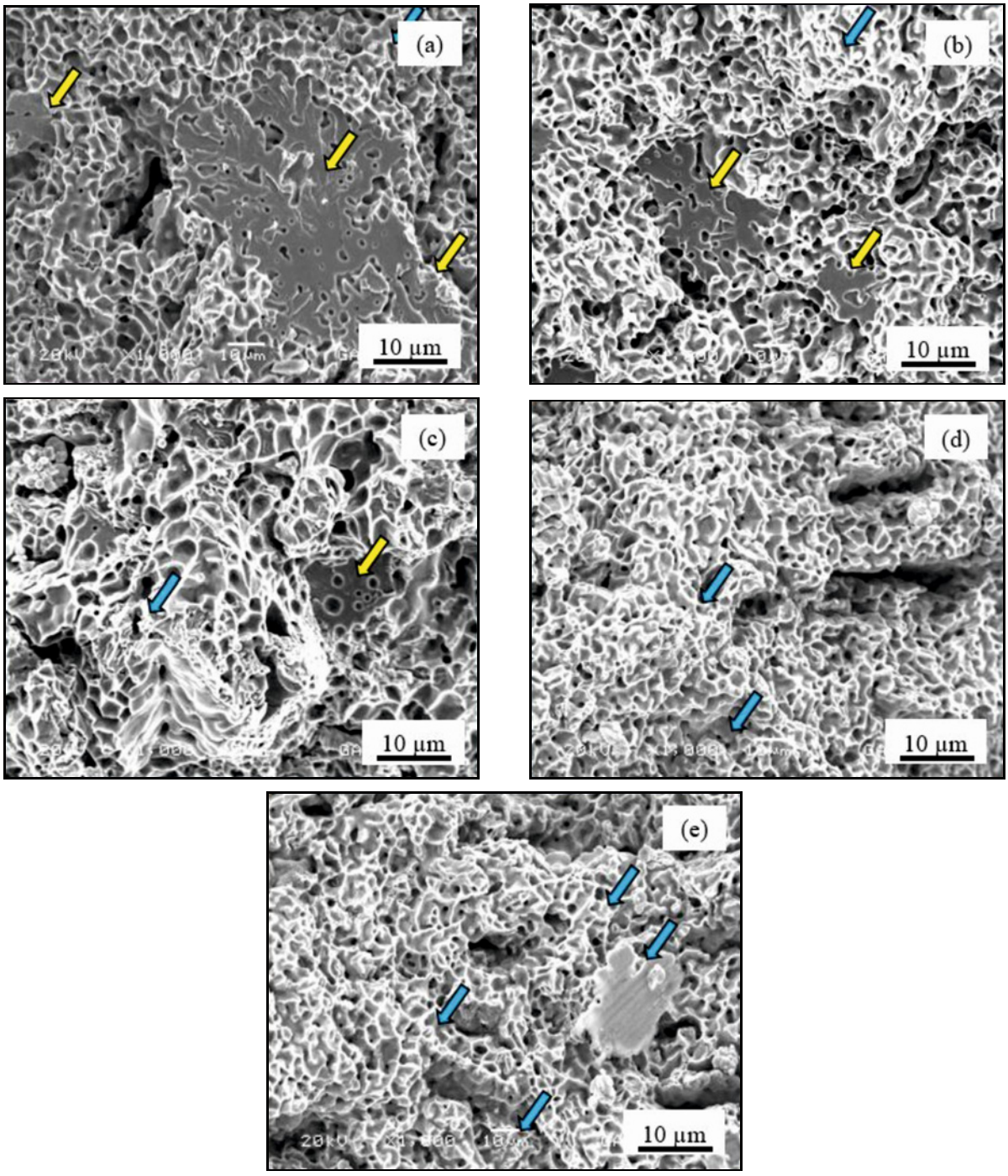

Fig. 9. Fractured surface SEM microstructures after impact test at 5 % by weight Ni at different temperatures: (a) –40 °C, (b) –20 °C, (c) 0 °C, (d) 25 °C, and (e) 40 °C.

(Fig. 5d). Completely ductile rupture was observed in this sample at the test temperature of 40 °C in the parts indicated by the blue arrows (Fig. 5e).

The fracture surface images of the sample produced with the addition of 0.5 % nickel after the impact test at different temperatures are given in Fig. 6. Slight ductile ruptures are observed on the surface at –40 °C compared to the P/M sample without nickel addition. Again, the ductile rupture of the structure increased with the increase in temperature. The addition of nickel element increased the ductility of the structure and increased the impact toughness valueIn this sample, the cleavage fracture mode (indicated by yellow arrows) is partially seen at most at 0 °C due to nickel addition, while at room temperature it can be said that a completely ductile failure mode (indicated by blue arrows) occurs instead of cleavage fracture (Fig. 6d). In other words, it is understood that the

dominant ductile rupture temperature decreases with the addition of nickel. This means that with the addition of nickel, the samples will have more toughness properties with lower temperature.

As can be seen in Figs. 6–9, with the further increase of nickel addition, the ductile rupture modes that contribute to the toughness resistance even at sub-zero temperatures have become evident. However, in the samples with 1 and 2 % nickel addition, even at –40 °C temperature, cleavage fracture is still very dominant (Figs. 7a and 8a), while it is seen that the cleavage fracture mode decreases significantly with the addition of 5 % nickel (Fig. 9a). The ductile fracture mode significantly increased with the addition of nickel in all samples with the increase in test temperature. The situation that causes ductile failure should be the formation of microvoids due to deformation, and sometimes microvoids coalesce at lower deformation rates to form the beginning of the crack. The energy required for such fracture must be damped by microvoids. It is important in terms of toughness resistance to delay the propagation of the cracks formed later from the cross-section plane or to change the crack propagation direction. Accordingly, it is thought that the nickel added in this study may have delayed the crack propagation. Since NRA's in regions with high nickel content are probably in FCC structure, it is thought that both the shear systems are more active and the dense atomic arrangement significantly reduces cleavage fracture [18–21].

The densities and types of phases that may occur as a result of the chemical interaction of the precipitated phases in the samples produced by adding different amounts of nickel to P/M steels with a carbon content of 1.2 % by weight were investigated by XRD analysis. In the XRD graph of P/M steel without nickel addition with 1.2 wt.% carbon, the cubic Fe element peaked in the (110) plane with the highest intensity at the angle of 44.60 2θ, and it also gave the second peak in the Fe (200) plane at the angle of 64.67 2θ (Fig. 10).

It was observed that the precipitated phases and peak levels changed with the increase in the doped nickel ratio. With the increase of the nickel ratio, the cubic Fe peak is obtained in the (110) plane at the highest peak intensity, while the higher number of cementite (Fe_3C) peaks are also present. It was observed that the intensity of the cementite peaks decreased with the increase of nickel addition, and the peaks of the nickel-containing austenite phase increased [21].

4. Conclusions

The results of the impact toughness properties of high carbon P/M samples with different nickel contents at different temperatures are provided as follows.

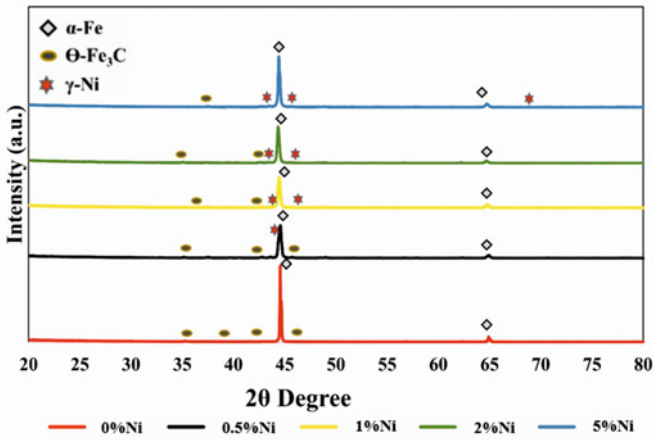

Fig. 10. XRD plot of the effects of different nickel addition rates on the crystallography of P/M steels.

1. With the increase in the amount of nickel content in P/M steels, the macrohardness (HV2) values at room temperature and –40 °C also increased. While the hardness value of P/M steel without nickel was 84 HV2, the hardness value of steel containing 5 % nickel element by weight was measured as 186 HV2 by increasing 121 %.

2. Impact toughness energies at each temperature increased with increasing nickel ratio. While the impact toughness of P/M steel without nickel was 17.3 J at room temperature, the impact toughness energy of the sample containing 5 % nickel element increased by 247 % and was measured as 45.75 J.

3. With the increasing nickel addition rate in P/M steel, the nickel-rich areas in the microstructure expanded and the pearlite colony sizes were shortened.

4. After the impact toughness tests at all temperature ambient with the increase in the nickel content on the fracture surfaces of the samples, dense dimple failure was observed instead of brittle fracture.

Acknowledgement

This work has been supported by Gazi University Scientific Research Projects Coordination Unit under grant number FYL-2021-7100.

References

[1] F. Bernier, P. Plamondon, J. P. Bailon, G. Esperance, Microstructural characterisation of nickel rich areas and their influence on endurance limit of sintered steel, Powder Metallurgy 54 (2011) 559–565. http://doi.org/10.1179/1743290111Y.0000000006

[2] P. Ramakrishnan, Automotive applications of powder metallurgy, in: I. Chang, Y. Zhao (Eds.), Advances in

Powder Metallurgy: Properties, Processing and Applications, Woodhead Publishing, Cambridge, UK, 2013, pp. 493–495.
[3] Höganäs AB, Höganäs Handbook for Sintered Components – Design and Mechanical Properties, Höganäs AB, 2015, p. 49.
[4] D. R. Askeland, P. P. Fulay, Essentials of Materials Science and Engineering, Nelson Education, Toronto, 2009. ISBN-13: 978-0-495-24446-2
[5] W. D. Callister, D. G. Rethwisch, Materials Science and Engineering, Wiley, New Jersey, 2013. ISBN-13: 9781119321590
[6] S. Tekeli, A. Güral, Effect of intercritical annealing and quenching plus tempering heat treatments on microstructure of Ni added powder metallurgy steels, Metarials and Design 28 (2007) 1353–1357. https://doi.org/10.1016/j.matdes.2006.01.022
[7] K. S. Hwang, M. Y. Shiau, Effects of nickel on the sintering behavior of Fe-Ni compacts made from composite and elemental powders, Metallurgical and Materials Transactions B 27 (1996) 203–211. http://doi:10.1007/bf02915046
[8] V. Tracey, Nickel sintered steels-developments, status and prospects, Metal Powder Report 47 (1992) 49. https://doi.org/10.1016/0026-0657(92)90907-V
[9] B. A. Gething, D. F. Heaney, D. A. Koss, T. J. Mueller, The effect of nickel on the mechanical behavior of molybdenum P/M steels, Materials Science and Engineering A 390 (2005) 19–26. https://doi.org/10.1016/j.msea.2004.05.087
[10] M. W. Wu, L. C. Tsao, G. J. Shu, B. H. Lin, The effects of alloying elements and microstructure on the impact toughness of powder metal steels, Materials Science and Engineering A 538 (2012) 135–144. https://doi.org/10.1016/j.msea.2011.12.113
[11] M. Nabeel, R. Frykholm, P. Hedström, Influence of alloying elements on Ni distribution in PM steels, Powder Metallurgy 57 (2014) 111–118. https://doi.org/10.1179/1743290113Y.0000000078
[12] N. Ridley, M. A. Malik, G. W. Lorimer, Partitioning and pearlite growth kinetics in an Ni-Cr eutectoid steel, Materials Characterization 25 1990 125–141. https://doi.org/10.1016/1044-5803(90)90025-F
[13] J. S. Park, H. G. Seong, J. Hwang, S. J. Kim, Adverse effects of Ni on the mechanical and corrosion-induced hydrogen embrittlement properties of ultra-strong giga steel used for automotive applications, Materials & Design 193 (2020) 108877. https://doi.org/10.1016/j.matdes.2020.108877
[14] U. Hildebrandt, W. Dickenscheid, Plasticity and alloy-softening in iron-nickel-alloys, Acta Metallurgical 19 (1971) 49–55. https://doi.org/10.1016/0001-6160(71)90160-X
[15] W. D. Callister, An Introduction: Material Science and Engineering. New York, 2007, pp. 106–139.
[16] S. I. Baik, R. K. Gupta, K. S. Kumar, D. N. Seidman, Temperature increases and thermoplastic microstructural evolution in adiabatic shear bands in a high-strength and high-toughness 10 wt.% Ni steel, Acta Materialia 205 (2021) 116568. https://doi.org/10.48550/arXiv.2010.09980
[17] S. Yaochen, L. Zeqi, Y. Chunmei, Y. Xuelian, K. Ying, Effect of alloying elements Cu and Ni on mechanical properties of steel/aluminum laser welded joints, Optic 255 (2022) 168707. http://doi.org/10.1016/j.ijleo.2022.168707
[18] D. Wang, Q. Zhong, J. Yang, S. Zhang, The influence of Ni on the microstructure and corrosion resistance of high-strength low alloy steel in the Cl-containing environment, Anti-Corrosion Methods and Materials 69 (2022) 9–16. http://doi.org/10.1108/ACMM-04-2021-2470
[19] K. Moeinfar, F. Khodabakhshi, S. F. Kashani-Bozorg, M. Mohammadi, A. Gerlich, A review on metallurgical aspects of laser additive manufacturing (LAM): Stainless steels, nickel superalloys, and titanium alloys, Journal of Materials Research and Technology 16 (2022) 1029–1068. http://doi.org/10.1016/j.jmrt.2021.12.039
[20] G. Altuntaş, O Altuntaş, M. K. Öztürk, B. Bostan, Metallurgical and crystallographic analysis of different amounts of deformation applied to hadfield steel, International Journal of Metalcasting 17 (2023) 1340–1349. http://doi.org/10.1007/s40962-022-00860-3
[21] M. S. Khan, A. Ghatei-Kalashami, X. Wang, E. Biro, Y. N. Zhou, Refining the hierarchical structure of lath martensitic steel by in situ alloying with nickel: morphology, crystallography, and mechanical properties, Journal of Materials Science 57 (2022) 1–28. http://doi.org/10.1007/s10853-022-07916-z